

## Behavior of a large concrete dam due to an actual maximum credible earthquake

M.T.Ahmadi

*International Institute of Earthquake Engineering and Seismology, Tehran, Iran*

Gh. Khoshrang, A. Mokhtarzadeh & A. Jalalzadeh

*Mahab-Ghodss Consulting Engineers, Tehran, Iran*

**ABSTRACT:** Due to the devastating M 7.6 earthquake of June 20, 1990 which occurred in Iran, a high concrete buttress dam located near the epicenter was severely shaken with intensity X. A two stage horizontal crack was formed at working joint levels in the central monoliths. The crack penetrated throughout the dam thickness causing severe leakage, but with no general failure. In this study the cause of such failure is elaborated using the estimated seismic load which coincides with the maximum earthquake of the site. An accurate dam-reservoir-foundation dynamic model is employed, with which detection of the actual crack location is made possible. A nonlinear pseudostatic analysis is also carried out and proved unable to predict the prototype behavior. The results has been utilized to effectively justify the repair techniques.

### 1 INTRODUCTION

Sefidrud concrete buttress dam was built during the period of 1958-1962 on a river of the same name in the northern Iranian province of Gilan. Its maximum height and crest length are 106 and 425 m respectively. It is composed of 30 (7 gravity and 23 massive head buttress types) monoliths 14 metres long each. Monoliths are 14 m wide at the upstream deck and 5 m thick at the buttress web. There is a transition (corbel) part connecting the web to the upstream deck. The footing of the high monoliths is 6 metres wide with 8 metres height. The crest elevation and the normal water level are at 276.25 and 271.65 m above the sea level correspondingly. This dam is constructed of plain concrete on a foundation material of Andesite and Basalt. Its reservoir is more than 1,700 million cubic metres in volume and is vital for irrigating the vast rice fields in the downstream. The dam had been originally designed with a seismic coefficient of 0.25g.

An exceptional strong ground motion in the seismotectonic province of Alborz in northern Iran occurred on June 21 (local time), 1990. Its magnitude is estimated between 7.6 to 7.7 in surface wave scale. The epicenter of the catastrophic earthquake which devastated the two large cities of Manjil and Rudbar was only about 5 kilometers far from the dam.

No recording of the ground motion or the structural response was obtained in the site. The nearest accelerograph, 40 km farther, recorded peak ground acceleration as high as 0.56g. The reservoir level was at elevation 265 when the earthquake caused heavy damages

to many concrete lift joints at the upper quarter of the dam specially in the central monoliths (Figure 1). Shear failures were visible in some cracks (marked by a, b, and c in Figure 2) resulting in horizontal 20 mm translation toward downstream and leaving the crack open due to aggregates dislocations which consequently caused severe leakage. This is the main damage suffered by the central monoliths and is composed of two horizontal cracks (a, and e) at elevations 258.25 (below the slope discontinuity i.e., the downstream kink) and 262.25, crossed by two oblique cracks (b-c, and d). In shorter monoliths near the abutments the main crack is formed from the downstream side. Extensive damage was also inflicted to the contraction joints. This includes concrete local crushing at different elevations and severe leakage from between two high monoliths inside the grouting gallery. The complete to partial destruction of the reinforced concrete parapet at the dam crest was also observed. Although the general structural stability of the dam was not found a matter of concern but immediate lowering of the reservoir elevation was decided as a preventive measure against the huge water leakage and the instability risks imposed by strong frequent aftershocks.

Phenomena of this type although not as intensive as in Sefidrud, might be recalled. In 1962 the Hsinfengkiang 105 m high diamond head buttress dam suffered a long crack at its downstream kink about 16 m below the crest due to a reservoir induced earthquake of M6.1 (Shen, et al. 1974). In 1967 a horizontal crack at the downstream kink (36.5 m below the crest level) of the 103 m high Koyna gravity

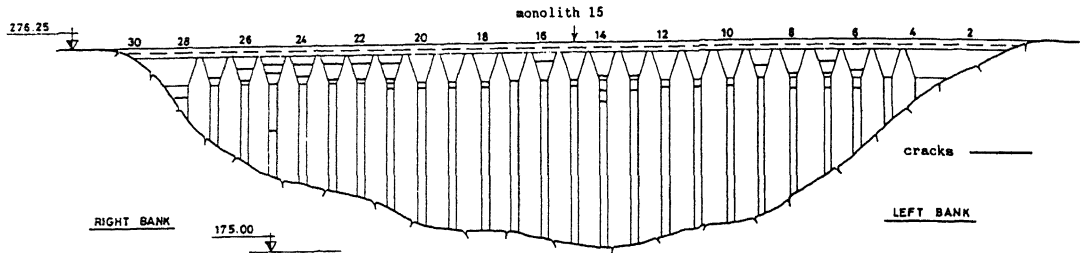


Figure 1. Downstream view of the cracked dam after the 1990 Earthquake.

dam occurred due to a near field earthquake of M6.5. The horizontal peak ground accelerations were 0.63g and 0.49g for the cross-canyon and stream directions respectively (Chopra & Chakrabarti 1972).

Although buttress dams are believed to be very vulnerable to cross-canyon earthquake motion, in the case of Sefidrud it is understood from the crack pattern that the earthquake stream direction component should be mainly responsible. Therefore the hydrodynamic action should have been definitely influential.

Nonlinear seismic behavior study of concrete gravity dams using model tests (Hall 1988), and mathematical simulations (Vargas-Loli & Fenves 1989) show that in most cases particularly when the hydrodynamic interaction is consistently included, the tensile cracks start from around the slope discontinuities of the faces. However still there are no actual verification of the crack extension pattern suggested by such models. There are still certain difficulties to account for the working joints which are planes of weakness. Besides the post-cracking shear strength of mass concrete, its shrinkage, and temperature effects are not well known yet.

In this work with the help of available strong motion data and site observations the seismic load and its predominant components are estimated first. Then an extensive analysis is performed to investigate the cause and mechanism of the cracks. Having verified the accuracy of the method, the repair techniques are examined by it.

## 2 THEORY

According to the above observations the practically infinite reservoir is essentially included. The compressibility of water is also accounted for. Moreover it is well known that the sediments at the reservoir bottom prevent resonance (Hatano 1949-1950), and thus their effect as a partial energy absorbing system specially for the case of Sefidrud, famous for its heavy sedimentation is also considered. Free surface gravity waves have been also accounted for. Non-reflecting viscous boundary conditions are employed in

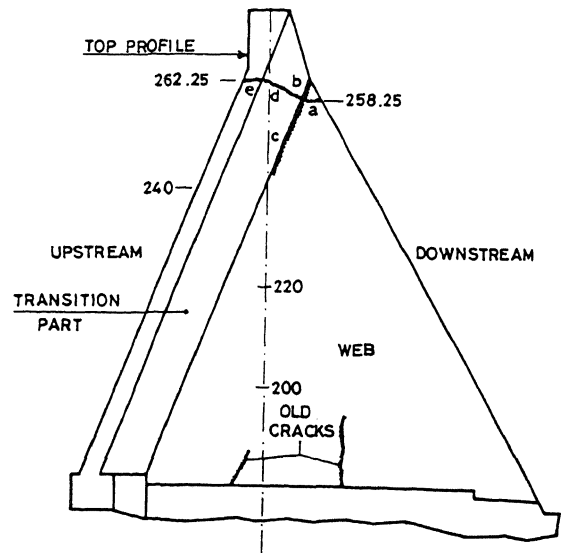


Figure 2. Crack map of monolith 15.

an efficient way to enable the absorption of the S, and the P waves at the foundation boundaries. The formulation is exclusively based on the displacement function as the unknown in all domains (Wilson & Khalvati 1983). The severe shortcomings of the approach in the fluid-structure interface is overcome by novel usage of surface elements with particular constitution and it is successfully verified by site observations and other mixed methods of hydrodynamic interaction analysis (Ahmadi & Ozaka 1988). Displacements are assumed as small everywhere. In dynamic analysis the equation of motion for the whole Lagrangian system is

$$K a + C \dot{a} + M \ddot{a} = f(t) \quad (1)$$

Here K, C, and M are the system stiffness, damping and mass matrices each composed of contributions from the structure, the fluid, the foundation, and the fluid-structure interface. Vectors a,  $\dot{a}$ , and  $\ddot{a}$  are the relative displacement, velocity, and acceleration. f(t) is the dynamic force.

The element shape functions of the structure and the fluid are essentially based on 22-node and 27-node elements respectively in order to have a balanced and compatible formulation. For fluid elements reduced quadrature is used. Very high rotational stiffness (100 times the bulk modulus of water) and a penalty function formulation are also employed to guarantee the irrotational motion.

The fluid-structure interface elements are 9-noded surface type with normal theoretically infinite elastic coefficients to avoid relative normal motion. However zero tangent elastic coefficient have to be employed to allow slipping between the fluid and the solid domains. An important component of Equation (1) is the non-proportional damping matrix  $C$ , which is composed of the contributions of the material damping, the reservoir upstream radiation boundary, the reservoir bottom absorption, and the foundation radiation boundary. The diagonalized consistent mass matrix is adopted. The seismic load vector  $f(t)$ , is expressed simply in a standard manner as a structural load for the multi-component earthquake.

Equation (1) could be solved for the system using direct time integration with the Newmark scheme. Modal analysis is not applicable due to the involvement of non-proportional damping and the "hourglass" modes coherent with the Lagrangian formulation. Thus the history of stresses could be calculated under the actual seismic event. The computer program SPRAD (Ahmadi & Ozaka, 1988) has been employed throughout the analysis.

### 3 MODEL

As a prototype of high monoliths, buttress no.15, one of the most damaged ones in the central part of the dam with 106 m height, is chosen for analysis. The interfaces between adjacent monoliths are considered motionless. This issue is also applied to the left and right faces of the foundation model. The dam consists of 44 three-dimensional 22-node isoparametric elements forming a single layer of elements in the dam axis direction. The foundation model consists of a slice of a half cylinder whose axis is parallel to that of the dam. Its radius is 1.2 times the monolith height. There are 36 three-dimensional isoparametric 20-node elements used in the foundation. In static analysis the foundation boundary nodes are fixed, but in dynamic analysis special radiation conditions are prescribed at these points. The reservoir finite element model consists of 24 three-dimensional 27-node elements. The reservoir length is twice its depth. For the fluid-structure interface 8 three-dimensional isoparametric 9-node elements are employed. The model is illustrated in Figure 3.

Concrete unit weight is 22.94 kN/m<sup>3</sup>, poisson ratio is 0.17, and the modulus of elasticity

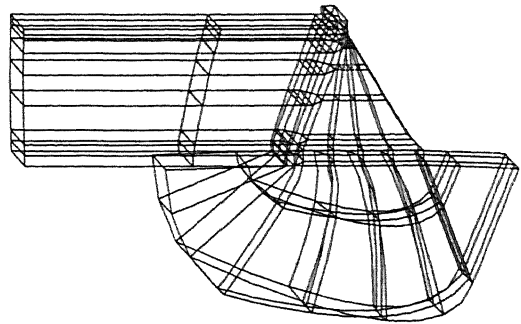


Figure 3. Finite element model of the dam-reservoir-foundation system.

is 20 GPa. The latter value is increased by 47% for dynamic analysis. The uniaxial compressive strength is found about 16.5MPa for cylindrical sample. As for the rock, four types of material with moduli of elasticity of 20., 12., 6., and 1.75 GPa are present in the foundation of monolith 15. The corresponding poisson ratios are 0.16, 0.17, 0.2, and 0.15 respectively. The rock moduli of elasticity are increased by 25% for dynamic analysis. The velocity of sound in water is 1440 m/sec. The bottom reflection coefficient for the old reservoir is determined equal to 0.67. The internal damping ratio is 5 percent.

### 4 LOADS FOR LINEAR ANALYSIS

Static loads comprise the gravity load which is applied only to the dam body, the hydrostatic pressure load (with normal water level of the reservoir), the jack force of 275MN in an oblique direction at the dam toe, and the uplift load which acts on about the half length of the dam bottom surface near its heel. The uplift pressure load is upward with a maximum intensity of 1. MPa at the upstream edge and a triangular distribution. This is decided based on the post-earthquake pressure measurement below monolith 15. Thermal and silt loads are not considered influential at the time of earthquake.

As for the dynamic actual load, the uncorrected peak ground accelerations of the 15 available accelerograms (Moinfar & Naderzadeh 1990) are used to assess the peak value at the dam site assuming the Gutenberg-Richter attenuation formula which lead to 0.714g for the horizontal peak value. Thorough investigations (Ministry of Energy 1991) has shown that the maximum credible earthquake of the site has the probable magnitude of 7.8 Richter, which is somewhat the same as the 1990 event. Moreover the prescribed site response spectrum as seen in Figure 4 is apparently in close agreement with that of the Abbar accelerogram which is the most intensive record of the 1990 event collected from rock base at a distance of

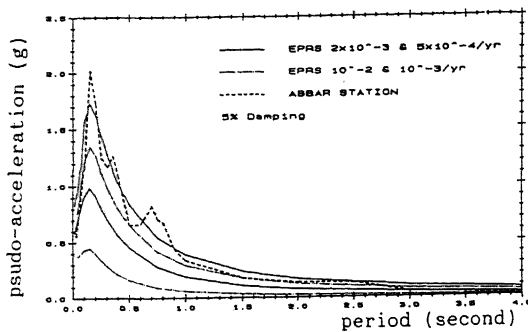


Figure 4. MCE and Abbar original response spectra (Ministry of Energy 1991).

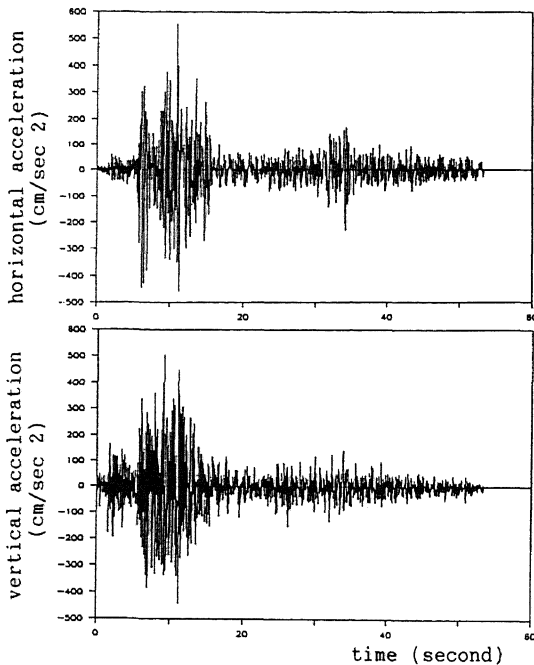


Figure 5. Original corrected accelerograms of Abbar recorded during the earthquake of 1990.

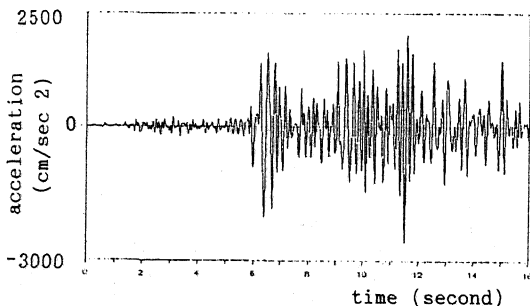


Figure 6. Relative horizontal acceleration response of node 454 (14 metres below crest) due to the scaled ground motions of Abbar records.

about 40 km far from the dam site.

Thus the horizontal component of the latter record is scaled for 0.714g, and its simultaneous vertical component is also normalized as to conserve the original ratio of the peak values of the vertical and horizontal components of the record. Hence the vertical component which is surprisingly intensive, has a peak value of 0.643g. The first 16 seconds of both components are used (Figure 5).

## 5 PSEUDOSTATIC SEISMIC LOAD FOR NONLINEAR ANALYSIS

In pseudostatic analysis to account for the effective persistent level of the ground acceleration, the horizontal peak value (0.714g) is reduced by a stochastic factor (Milutinovic & Kameda 1983) which is usually less than unity (here 0.58). Based on this reduction for the maximum earthquake, and using the gravity dam simplified earthquake analysis method (Fenves & Chopra 1987) a vertical distribution of the relative acceleration is obtained ranging from a maximum approximate value of 1.4g at the top to zero at the bottom. According to the latter non-uniform acceleration the maximum hydrodynamic pressure is obtained using the Westergaard formula based on the local structural acceleration values.

## 6 NUMERICAL RESULTS

### 6.1 Verification of the dam behavior

In order to check the behavior of the proposed model and the actual dam, a linear dynamic analysis as well as a pseudostatic nonlinear analysis are conducted.

#### 6.1.1 Linear analysis

In Figure 6 the relative acceleration response time history is plotted. In general concrete dams are known to amplify the ground motions several (3 to 7) times on the top (Ahmadi & Ozaka 1988) and this has eventually lead to the destruction of the top profile and the parapet at the dam crest. This amplification is overlooked in uniform pseudostatic seismic analysis causing great underestimation of the stresses. Figure 7 illustrates the maximum tensile total (static plus dynamic) stresses and their associated principal components. These stress crosses do not necessarily occur simultaneously. The extreme value of these tensile stresses in the dam body (5.0 MPa) has happened about 4 metres below the downstream kink that is exactly at the actual main crack location. The direction of this stress is parallel to the web face slope i.e., almost normal to the construction joints. Thus

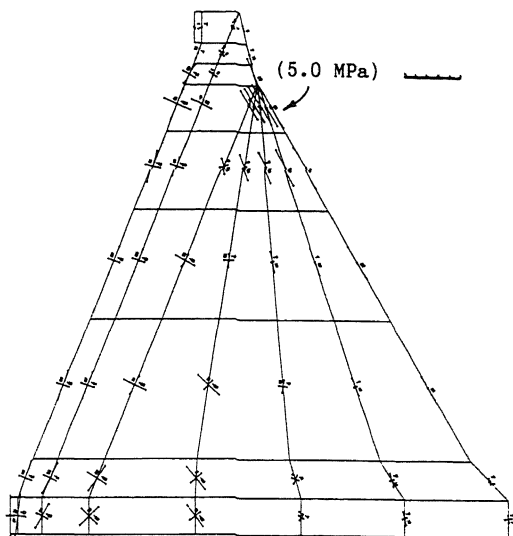


Figure 7. Total principal stress crosses corresponding to the maxima of tension due to the scaled ground motions of Abbar records.

spectacular coincidence of the computational results and the actual phenomenon is evident. It is very interesting to notice the high similarity of the maximum tensile stress distribution pattern at higher elevations due to different input motions of the same event. Figure 8a corresponds to response due to the input motion of another record (Ghazvin, at 60 km far from the dam site) for a rigid foundation model, whereas Figure 8b is related to the case of Abbar. The dissimilarities in the bottom stress conditions are attributed to the different models of the foundation.

These magnitudes of tensile stress are far higher than the dynamic tensile strength of the concrete joints. And as seen before, the direction of tension is approximately normal to the weak horizontal planes formed by these joints. Thus it could be concluded that tensile crack might have been initiated from the point at elevation 258.25 on the downstream face.

In contrast to the tensile stress it was observed that the extreme total compressive stresses ever-experienced by high monoliths is only 6.9MPa which is far lower than the concrete compressive strength (about 16.5 MPa), and therefore compressive failures and crushing are believed as improbable.

These considerations reveal that the linear analyses findings and results are consistently in agreement with the actual phenomenon and the model should be quite reliable for the study of rehabilitation techniques.

#### 6.1.2 Discussion

After a tensile failure at elevation 258.25 in

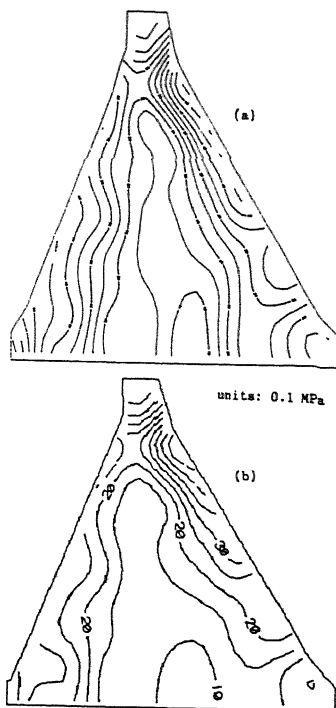


Figure 8. Contours of maximum total tensile stresses for (a) rigid foundation model due to the Ghazvin records, and (b) flexible foundation model due to the Abbar records

the downstream face the followings might have occurred:

The sequence of impacts in the initial tensile crack (designated by "a" in Figure 2) induced the shear crack "b". This is followed by the new shear crack "c" at the conjunction of the web and the transition part due to the dynamic shear flow between the buttress web and its head. Then cyclic motion has gradually pushed the separated wedge-shape concrete block outward.

Therefore the top profile reduced to the buttress head which could be called a trapezoidal section cantilever with oblique axis. Naturally the dynamic maximum flexural tensile stress at the trapezoidal section corresponds to its thinner side i.e., on the downstream side at elevation 258.25. From here the crack crossed the "cantilever" perpendicular to its oblique axis toward the upstream face. There, it met the weak plane of working joint at 262.25 in which a partial crack might have already occurred at the upstream face. This discussion seems true for most of the cracked monoliths.

#### 6.1.3 Nonlinear pseudostatic analysis

A nonlinear analysis is conducted with the

psudostatic seismic loads defined in section 5, plus static loads of section 4. The tensile strength criterion is adopted along with discrete crack elements at pre-defined potential crack surfaces (Ahmadi & Razavi 1992). A new mesh had to be constructed in order to conform with the actual crack map. The new mesh consists of 56 three-dimensional 20-node brick and twelve 8-node surface elements. The foundation is not included. Upon the occurrence of tensile stress beyond a certain limit (here 1.1 MPa) a tensile crack would occur in the pre-defined surface. Otherwise the material is completely elastic. The shear, and normal elastic coefficients of the weak surface are adopted equal to 200 and 16 GPa/m respectively. Direct iteration scheme which essentially converges to a lower bound solution of the failure condition is applied. The maximum compressive and tensile stresses are 7.2MPa and, 1.1 MPa respectively both in the foundation contact area. Noticeable is the joint opening (or tensile failure) location formed at the foundation interface rather than in the top profile. Thus the result does not conform with the prototype when even such refined psudostatic analysis is carried out.

## 6.2 Evaluation of the rehabilitation procedure

As the main crack is initiated by tensile stresses and followed by the shear action, a vertical compressive mean prestress of about 0.8MPa (at the crest elevation) by 12 post-tension VSL type tendons of 40 metres length, was proposed by the dam designer. This was supposed to reduce the tensile seismic stress and supply the frictional shear resistance. A resin injection to fill the highly porous and cracked zones was also prescribed. The satisfaction of the above requirements are verified for the Design Basis Earthquake (DBE) (Ministry of Energy 1991), while cables included. It is realized that the maximum instantaneous total tensile stress will be less than 2.5MPa within the 40 metres of the uppermost part of the dam, i.e., where cables are included. The dynamic tensile strength of the joints is believed to be around the latter value. It is also observed that in the lower parts the maximum tensile stress does not exceed 1 MPa which ensures high safety.

Furthermore psudostatic stability analyses of the top profile due to the maximum acceleration and hydrodynamic pressure modified by the reduction factor of section 5, plus static loads, reveals that the factors of safety against overturning and sliding are quite satisfactory, for both the MCE, and the DBE cases. Moreover A check on the level of cable strains during the DBE is conducted at different sections. Safety against yielding could be achieved only when the tendons are unbonded, and strain averaging is admitted.

## 7 CONCLUSION

The results of analyses conducted here using the actual records of the near-field maximum credible earthquake as the inputs, effectively match with the real phenomenon only when the consistent formulation of the dam-reservoir interaction is employed. Nonlinear refined psudostatic analysis is found unable to predict the phenomenon. The tensile crack followed by shear crack is explained intuitively. Based on extensive analyses the proposed repair measures are evaluated.

## 9 REFERENCES

- Ahmadi, M.T. & Y. Ozaka 1988. A simple method for the full-scale 3-D dynamic analysis of arch dam. Proc. 9th WCEE 6; 373-378.
- Ahmadi, M.T. & S. Razavi 1992. A three-dimensional joint opening analysis of arch dam. Comp.Struct. to be published.
- Chopra, A.K. & P. Chakrabarti 1972. The earthquake experience at Koyna dam and stresses in concrete gravity dams. Earthquake Eng.Struct.Dyn. 1; 151-164.
- Fenves, G. & A.K. Chopra 1987. Simplified earthquake analysis of concrete gravity dams. J.Struct.Eng. ASCE 113(8); 1688-1708.
- Hall, J.F. 1988. The dynamic and earthquake behaviour of concrete dams: Review of experimental behaviour and observational evidences. Soil Dyn. Earthquake Eng. 7; 57-121.
- Hatano, T. 1949-1950. Accurate solution of dynamic water pressure on dams during earthquakes (in Japanese). Proc. JSCE 3; 174-183.
- Milutinovic, Z. & H. Kameda 1983. Equivalent ground acceleration (EQA) as an engineering seismic hazard parameter. Research Report 83-ST-01, School of Civil Engineering, Kyoto University, Japan.
- Ministry of Energy 1991. Rehabilitation study of Sefidrud dam; report on the seismicity and seismic hazard of the dam-site. Mahab-Ghodss Consulting Engineers, Tehran.
- Moinfar, A.A. & A. Naderzadeh 1990. An immediate and preliminary report on the Manjil, Iran earthquake of 20 June, 1990. Publication 119, Building and Housing Research Center, Tehran.
- Shen, C., H. Chen, C. Chang, L. Huang, T. Li, C. Yang, T. Wang, & H. Lo 1974. Earthquakes induced by reservoir impounding and their effect on Hsifengkiang dam. Scientia Sinica 17(2); 239-272.
- Vargas-Loli, L.M., & G.L. Fenves 1989. Effects of concrete cracking on the earthquake response of gravity dams. Earthquake Eng. struct.dyn. 18; 575-592.
- Wilson, E.L., & M. Khalvati 1983. Finite elements for the dynamic analysis of fluid-solid systems. Int.J. Numer. Meth. Eng. 19; 1657-1668.